Exploring supramolecular interactions and architectures by scanning force microscopies

Paolo Samorì†[ab]

Received 3rd February 2005
First published as an Advance Article on the web 18th March 2005
DOI: 10.1039/b404021j

The development of new methodologies based on scanning force microscopy (SFM) has made it possible to map topographies, chemical functionalities, and numerous other physicochemical properties of complex assemblies, to unravel dynamic processes, to measure forces generated along a reaction coordinate, to nanopattern surfaces and to nanomanipulate objects. This *tutorial review* highlights the most recent applications of these SFM-based capabilities, on and beyond imaging, to the exploration of supramolecular interactions and architectures, to the fabrication of smart materials and to the optimization of (nano)devices.

Introduction

Supramolecular chemistry, the 'chemistry beyond the molecule', provides direct access to complex architectures where the single molecular building blocks are held together by relatively weak non-covalent interactions such as hydrogen bonding, π–π stacking, electrostatic, and van der Waals interactions. Using nature as a source of inspiration, the generation of more and more complex self-organized architectures, with structural motifs controlled over a wide range of length scales, has recently become possible by applying the concept of hierarchical self-assembly, *i.e.* the non-covalent organization of (macro)molecules which takes places over distinct multiple levels. The generation of such organised structures, obtained by controlling supramolecular interactions, makes it possible to tune a large number of physico-chemical properties of molecular based materials.[1]

† Dedicated to Professor Jürgen P. Rabe on the occasion of his 50th birthday

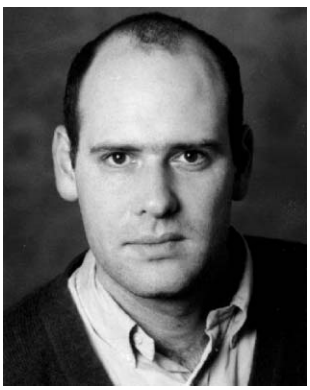

Paolo Samorì

Paolo Samorì (Imola, Italy, 1971) obtained his Laurea in Industrial Chemistry at University of Bologna. He took his PhD in Professor J. P Rabe's group (Humboldt University Berlin) on self-assembly of conjugated (macro)molecules at surfaces, then he was a postdoctoral student in the same lab. In 2001 he was appointed as a permanent researcher at ISOF-CNR (Bologna). Since 2003 he has been visiting professor at ISIS-ULP (Strasbourg). His present interests include self-assembly of hybrid architectures at surfaces, supramolecular electronics and fabrication of nanodevices. He received the graduate student awards at EMRS (1998) and MRS (2000), and the IUPAC Prize for Young Chemists (2001).

Until a few years ago, organic and biological thin films were visualized by means of optical and electron microscopies. While the former does not allow high spatial resolutions to be achieved, the latter can be applied only to electrically conductive samples. The electron microscopic imaging of soft insulating materials could be accomplished by coating the chosen sample with metals (*i.e.* staining), losing in this way structural details of the surfaces and altering their physico-chemical properties.

The invention of scanning tunneling microscopy (STM) in 1981 boosted the scope to nanoscale science and nanotechnology.[2] STM made it possible to gain insight into the structures and dynamics of thin films with sub-molecular resolution. Unfortunately, STM relies on the tunneling of electrons, hence it virtually cannot really be applied to thick insulating organic films. With the development of atomic force microscopy (AFM), known also as scanning force microscopy (SFM),[3] this limitation was overcome. By scanning a sharp tip on a surface while keeping constant the force between them, the surface topography of thick insulating organic and biological films deposited on a flat surface can be mapped. The SFM explorations can be made on length scales spanning from the hundreds of micrometres down to the nanometres, thus different levels of the hierarchical self-assembly can be explored. Moreover SFM can be employed under a variety of environmental conditions permitting the investigation of the dependence of physico-chemical properties of a given (supra)-molecular system on these conditions, which is one of the hallmarks of supramolecular chemistry. These SFM explorations can be applied also to dynamics phenomena, which can be studied in real-time.

This *tutorial review* directs the reader to several particularly remarkable and enlightening results obtained by exploiting SFM based techniques on supramolecularly engineered architectures. Due to the large number of works performed with these methods every achievement will not be treated extensively. This article is divided into four sections:

1. Visualization of supramolecular architectures and interpretation of the structural motifs;

2. Properties governed by supramolecular interactions, *i.e.* mechanical and electrical properties as well as phase segregation;

3. Determination of the strength and the nature of individual weak interactions;

4. Nanopatterning and nanomanipulation.

Visualization of supramolecular architectures and interpretation of the structural motifs

SFM is a key tool for the visualization of surfaces and interfaces with a spatial resolution down to the 1–3 nm scale, consequently it is an ideal technique to elucidate the molecular packing of self-assembled species. This can be accomplished by quantitatively estimating the dimensions of the nanostructures adsorbed at surfaces. The visualization of complex supramolecular architectures is facilitated by the isolation of the single nanostructure to be studied. Different weak interactions, including π–π stacking and H-bonding, make it possible to form quasi-1D self-isolated architectures, with molecular cross sections, which can be directly investigated with SFM. Other molecular systems are more prone to self-associate into less ordered arrangements. Nevertheless, their isolation can be achieved in 2D using a template monolayer, or even in 3D by chemical encapsulation.

Isolated nanostructures based on weak interactions

Supramolecular fibers from π–π stacked conjugated (macro)-molecules. Tapping-mode SFM,[6] which is a very poorly invasive methodology, was successfully used to visualize homopolymeric alkylated poly(*para*-phenyleneethynylene) (PPE) nanoribbons self-assembled by drop-casting a PPE solution onto the electrically insulating mica surface. These anisotropic architectures, which possess a molecular cross-section and a length of several micrometres, were oriented along the crystallographic axis of the mica crystalline surface (Fig. 1a). Notably, due to their sizes, direct information on the structure of such architectures cannot be obtained with conventional analytical methodologies. The ribbons consist of several rods assembled parallel to each other; each rod typically conveys two PPE molecules packed with the hexyl side chains oriented perpendicular to the basal plane of the substrate (Fig. 1c,d). The dominant type of intermolecular interaction between these conjugated (macro)molecules is π–π stacking.[4] Due to the occurrence of phase segregation in the polydisperse macromolecules occurring at surfaces, the ribbon's cross-sections are constant for hundreds of nanometres long segments. These highly ordered supramolecular nanostructures, after being doped, are promising candidates for the development of molecular nanowires to be interfaced to gold nanoelectrodes prepared by lithographic routes, *e.g.* E-beam lithography.

Analogous supramolecular nanoribbons were also formed both with block-copolymers based on a rod-like conjugated PPE (Fig. 1b), poly(*para*-phenylene) or poly(fluorene) segment covalently linked to flexible poly(dimethylsiloxane)

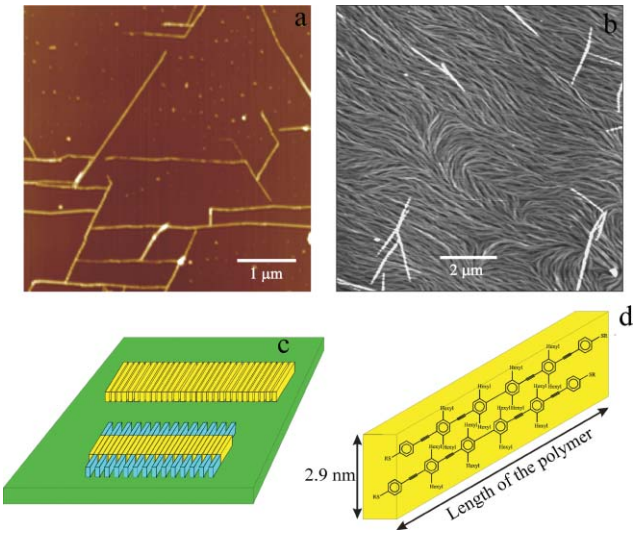

Fig. 1 Tapping-mode SFM topographical image of (a) poly(*para*-phenyleneethynylene) (PPE) nanoribbons self-assembled by drop-casting a PPE solution in a mixture of phenyloctane and THF onto a mica surface.[4] (b) poly(*para*-phenyleneethynylene)-*b*-poly(dimethylsiloxane) block copolymer ($(PE)_{12}$-b-$(DMS)_{15}$) physisorbed on mica from a solution in toluene.[5] (a) The average contour length of the macromolecule employed, as determined by ^{1}H-NMR analysis, is 7.9 nm. The vertical scale is 20 nm. These anisotropic architectures, which possess a molecular cross-section and a length of several micrometres, can be oriented along the crystallographic axis of the mica crystalline surface. (b) The average ribbon width corresponds to the average contour length of the copolymer. (c,d) Cartoon of the supramolecular arrangement forming the ribbon: (c) the ribbon consists of several rods assembled parallel to each other both in the case of the homopolymer (top) and in that of the copolymer (bottom); (d) in the case of the homopolymer, each rod typically conveys two PPE molecules packed with the hexyl lateral chains perpendicular to the basal plane of the substrate. (a,c,d) Reproduced with the permission of Wiley VCH (ref. 4)

or poly(ethylene-oxide) chains,[5,7] and very recently with an oligomeric PPE derivative.[8] Similarly, fiber-like objects with a molecular cross-section were produced by π–π stacking interactions from sexithiophene derivatives, such as 2,2′:5′,2″:5″,2‴:5‴,2:5,2⁗⁗-sexithiophene-5,5⁗⁗-dicarboxylic acid-(2*S*)-2-methyl-3,6,9,12,15-pentaoxahexadecyl ester. In this case a helical supramolecular architecture was produced thanks to the effect of the chiral units in the penta(ethylene glycol) segments attached to the α- and ω-positions of the main oligothiophene chain.[9] The growth into ribbons from a conjugated polymer was boosted by grafting crown ethers to poly(*para*-phenylenevinylene) chains (leading to C-PPV). In this case the self-assembly into nanoribbons due to π–π stacking was assisted by the interactions between the crown-ethers in the presence of K^+. The length of the nanoribbons increased with the standing time of the C-PPV/K^+ solution, although this approach did not allowed to control the ribbon cross-section at the single molecule level.[10]

Supramolecular fibers can also be produced by π–π stacking of 3D polyphenylene dendrimers[11] or 2D discotic units, *i.e.* phthalocyanines. These latter stacks, if obtained from

molecules properly functionalised with reactive units such as styryl groups, can be photopolymerized leading to 1D polymers.[12]

Supramolecular fibers based on H-bonding. SFM permitted the visualization highly anisotropic H-bonded networks of single[13] and double components.[14] While the first consisted of guanosine derivatives, the second was made from 5-(4-dodecyloxybenzylidene)-(1*H*,3*H*)-2,4,6-pyrimidinetrione and 4-amino-2,6-didodecylamino-1,3,5-triazine. These quasi-1D architectures possess lengths on the micrometre scale and a molecular cross-section. Hydrogen bonding can also be exploited to self-assemble giant supramolecular assemblies, *i.e.* hydrogen-bonded tetrarosettes, adsorbed on HOPG into 2D nanorod domains, which have been monitored with a molecular resolution. Two sets of domains with different mutual orientations were resolved, providing evidence for the presence of the racemic rosette mixture into enantiomerically pure domains on the substrate.[15]

Isolation of single molecules

The isolation of single molecules is a viable approach for their visualization. Physisorbed or chemisorbed self-assembled structures at surfaces can be exploited to form a molecular matrix which can host single molecules deposited from very diluted solutions. This has been done with dendrimers physisorbed at surfaces[11] or embedded (*i.e.* chemisorbed) in a self-assembled monolayer of thiol functionalized molecules covalently grown on Au.[17] Using the second method, coordination cages have been inserted in a 11-mercaptioundecanol SAM on Au. On these hybrid systems it has been possible to detect, from the height of the molecules in the SFM images, the occurrence at surfaces of a reversible process of assembly and di-assembly, from single cavitand to cage molecule (Fig. 2).[16]

A fine tuning of interfacial as well as intermolecular and intramolecular interactions permitted to grow ordered mono- and multi-component quasi-1D structures at surfaces which were visualized by SFM. Taking advantage of the known tendency of simple alkanes to physisorb on the graphite surface, alkyl substituted calix[8]arene derivatives bearing amide, urea and imide functions have been self-assembled on HOPG into tubular nanorods with a molecular cross-section *via* hydrogen bonds between *p*-amide units.[19] In a different set of experiments, surfactants bearing long aliphatic chains and polar head groups have been used to direct the growth of almost perfectly straight metallo-supramolecular coordination polyelectrolyte complexes on HOPG.[20] This surfactant templated self-assembly turned out to be a very general approach that can be applied to a variety of synthetic and biological systems. This has allowed very recently the stretching of dsDNA chains (Fig. 3),[18] as well as of more flexible macromolecules, allowing visualization in their fully extended conformation, and consequently quantitative determination of their contour lengths.[21] This made it possible to gain directly an absolute estimation of the mass distribution for a polydisperse molecular system such as polystyrene sulfonate.[21] Alternatively the determination of the molecular weight distribution of a polydisperse system from SFM data was also possible by quantitatively estimating the widths of the

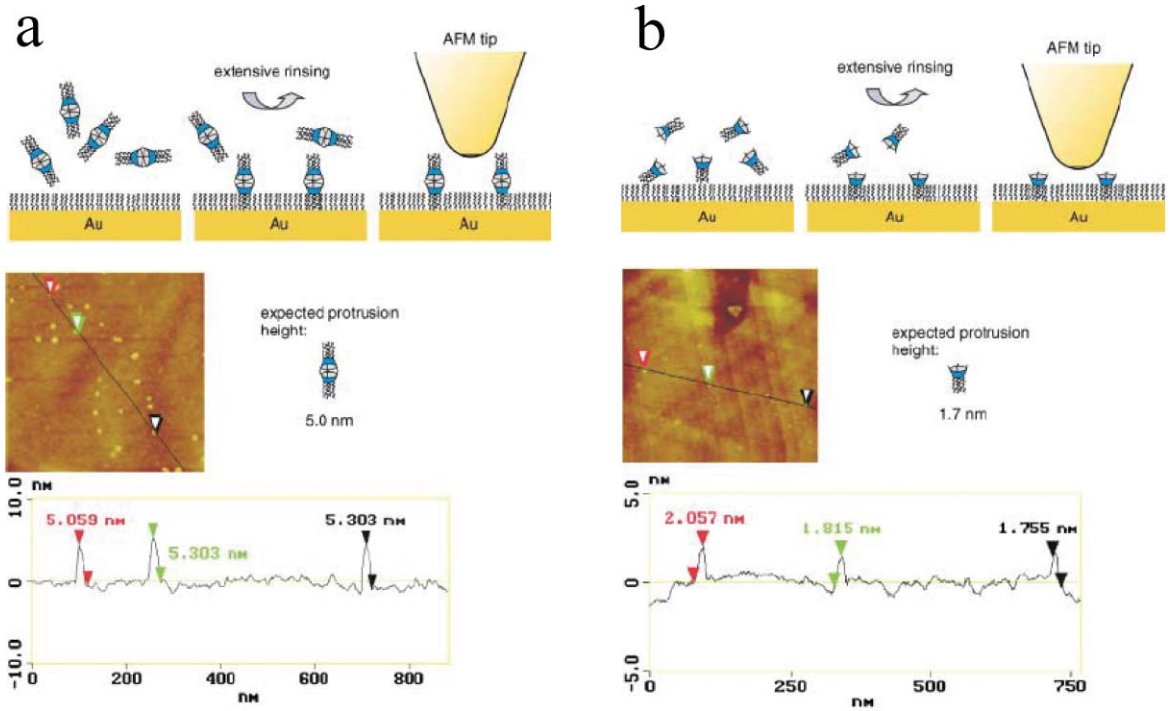

Fig. 2 (a) Cartoon of the insertion of a cage molecule in a SAM of 11-mercaptioundecanol (MU) on Au. TM-SFM topographical image and cross-section analysis of the cage inserted in the MU monolayer. (b) Schematic representation of the cavitand insertion in a MU SAM on Au. TM-SFM height image and section analysis of the MU monolayer with embedded a phenylpyrin functionalized thioether-footed cavitand.[16] Reproduced with the permission of Wiley-VCH.

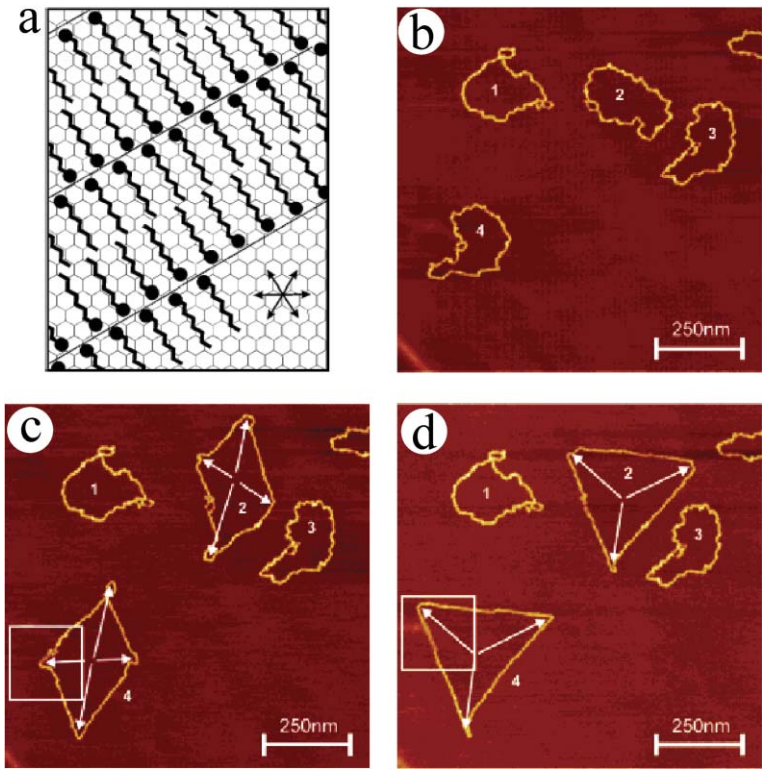

Fig. 3 (a) Scheme of a monolayer of alkane derivatives on HOPG. Black circles indicate polar headgroups and arrows denote the crystallographically equivalent graphite axes having three-fold symmetry. (b–d) TM-SFM topographical images of dsDNA adsorbed on a HOPG substrate modified with $CH_3(CH_2)_{11}NH_2$ molecules. Manipulation was performed by bringing the tip in contact with the surface and moving it in the desired direction. (b) ds-plasmid DNA molecules as deposited; (c) after stretching two of them (nos. 2 and 4) along the white arrows; (d) after manipulation of the same molecules into triangles.[18] Reproduced with the permission of the American Chemical Society.

previously described supramolecular PPE nanoribbons (see Fig. 1a).[4]

Encapsulation of single molecules

The supramolecular approach holds the potential to afford control over a number of physico-chemical properties of molecular species, including the structural, electronic and mechanical properties. Polyrotaxanes designed with a conjugated polymer backbone, as *p*-phenylene or fluorene type, inserted in a series of insulating α- or β-cyclodextrins (CDs), were found to possess unique properties if compared to the non-rotaxinated derivative. The rotaxination decreased the π–π interactions between the single conjugated macromolecules. While in the non-rotaxinated form the molecules self-assembled into layers at surfaces, in the rotaxinated derivatives isolated strands are adsorbed at surfaces. Noteworthy, the rigidity of the single chains is notably increased, as a result of the steric hindrance conferred by the macrocycles. This control over the structural properties at both the single and multi-molecule level gave also rise to unique optical and electronic properties, while preserving the intrinsic semiconducting properties of the chains. This allowed to achieve an increase in the luminescence efficiency and blue-shifted emission, as well as an enhanced environmental stability and a greater resistance to luminescence quenching by impurities.[22] In a similar approach, semifluorinated *n*-alkanes ($F(CF_2)_8$–$(CH_2)_{16}H$ have been encapsulated in β-CDs in an aqueous solution. This spontaneous self-assembly is due to the hydrophobic nature of alkanes which readily penetrate the hydrophobic CD's cavity, to avoid contact with water. SFM visualization revealed tubular structures with a constant cross-section obtained from dispersion of the ($F(CF_2)_8$–$(CH_2)_{16}H$)/β-CD inclusion compound, while X-ray diffraction showed that the host–guest system presents the channel type structure which is typical of polymer-CD inclusion compounds. The formation of such supramolecular assemblies may be useful for the encapsulation of fluorinated hydrophobic materials and for the insertion of a given polymer into the surface of cyclodextrin grafted fibers and textiles.[23]

Properties governed by supramolecular interactions

In addition to the capability of SFM based approaches to elucidate the structural motif of complex supramolecular architectures, they grant insight into different physico-chemical properties of the surfaces.

Mechanical properties of single macromolecules

SFM makes it possible to study conformational and mechanical properties of single (macro)molecules[24,25] or of supramolecular architectures.[9] Upon given conditions, single polymer chains can be equilibrated in quasi-2D on a surface as in an ideal "2D solution". The analysis of the SFM images recorded on these chains can be successfully used to estimate

the polymer persistence length (l_p) of the polymer, which is a direct measure of the average local conformation, *i.e.* rigidity, for a linear polymer chain. The obtained estimation on dsDNA was found to match the values obtained by indirect measurements in solutions.[26]

Synthetic polymers of isocyanodipeptides, when functionalized with sterically demanding side chains adopt a 4_1 helical conformation (four repeats per turn) which accounts for the relatively high stiffness of the polymer. By attaching L-alanyl-D-alanine methyl ester side groups in the side chains (Fig. 4a), the amide moieties in these pendant dipeptides self-associate into four hydrogen-bonded networks which are oriented parallel to the main chain of the polymer (Fig. 4b). This peculiar supramolecularly engineered design confers a notable stiffness to the overall chain. A tapping mode SFM study of the conformation of isolated macromolecules equilibrated at a surface revealed extraordinarily stiff chains on mica (Fig. 4c). The statistical analysis on the chains revealed a l_p of (76 $\pm$ 6) nm[27] which is more than one order of magnitude larger than the l_p determined in solutions for poly(isocyanides) that are not bearing the lateral hydrogen bonds, *i.e.* poly(α-phenylethylisocyanide).[27] This indicates that the hydrogen bonded networks existing in the side-chains of the polymers notably improve the mechanical properties of the polymer.

Similar improvement was accomplished on the aforementioned π-conjugated polyrotaxanes. The steric hindrance conferred by the CD macrocycles shielding the π-conjugated polymers has remarkably increased the stiffness of the strands.[22]

Electrical properties

Frisbie and co-workers have pioneered conducting-probe SFM measurements, which have made it possible to probe electrical properties of 2D nanostructures, such as oligothiophene layers,[28] SAMs of saturated alkanethiols, unsaturated carotene or oligophenylene SAMs chemisorbed on Au(111).[29] The advantages of using SFM, rather than STM-based approaches, include that: (i) SFM provides a true topographic map of the investigated nanostructure, (ii) it offers the possibility of studying samples that are highly resistive or surrounded by insulating regions, (iii) it permits the location of the electrode (SFM tip) in direct contact with the sample in a reproducible fashion.[29] The drawback of using SFM is the larger contact area in the electrical measurements. Furthermore, by using a Au nanocluster with a 1.5 nm diameter embedded between the conductive SFM probe and the SAM, one can reduce the effective contact area.[30] This valuable approach appears to be ideal to study the electrical properties of quasi-1D supramolecular "wires" such as the nanoribbons previously presented. Another approach that holds potential to gain important insight simultaneously into the electrical and morphological properties of supramolecular architectures self-assembled at surfaces is Kelvin probe force microscopy.[31] Such a technique makes it possible to determine the work function of nanostructures, thus it can be foreseen to be important in the field of nanoelectronics, aiming at improving the transport across a metal–organic junction which strongly depends on the tuning of the Fermi level of the metal with that of the organic active self-assembled structure.

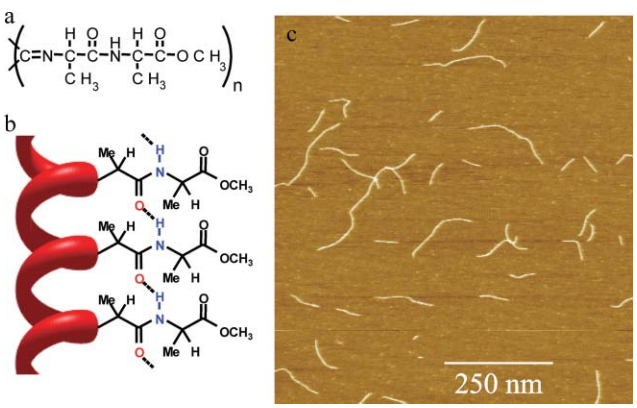

Fig. 4 (a) Chemical formula of the poly(isocyano-L-alanyl-D-alanine methyl ester) (PIC). (b) Hydrogen bonded array within the side chains of the polymer. (c) TM-SFM topographical image of a film prepared from a 0.001 g L^{-1} PIC solution in chloroform. *Z*-range: h = 2 nm.[27] Reproduced with the permission of the American Chemical Society.

Phase segregation

Phase segregation in macromolecular and surface chemistry is usually governed by the phenomenon of molecular recognition. Phase segregation can occur both in a polydisperse macromolecular system and in a multicomponent system. While in the former it consists of a macromolecular fractionation processes, in the latter different chemical species separate one another due to the occurrence of self-recognition processes. The self-assembled nanoribbons of the PPE based block-copolymer shown in Fig. 1b epitomize both of these two types of segregation processes.[5] The first type of segregation was also found in the homopolymeric PPE system (Fig. 1a). The conjugated polymer self-segregates into ribbons possessing segments with a constant cross-section. In this case the single chains adopt a fully extended conformation and are oriented perpendicularly to the long ribbon axis, leading to single-molecule wide ribbons.[4] The second type of phase segregation, observed only in the block-copolymer derivatives, consisted in the separation between the rod-like conjugated PPE segments from the flexible poly(dimethylsiloxane) counterparts. Only for block copolymers bearing a long conjugated segment, π–π stacking governs the self-assembly into nanoribbons,[5] as those obtained with the homopolymeric compound.

Strength and nature of individual weak interactions

In order to explore "molecular sociology", *i.e.* how different molecules interact and associate, it is of prime importance to be able to get insight into the nature and the strength of weak bonds. The invention of chemical force microscopy (CFM) paved the way towards this assessment since it combines (i) the force sensitivity of the SFM (down to the sub-nanonewton or even piconewton scale), (ii) the spatial resolution of SFM (sub-nanometre) and (iii) the chemical discrimination. In the pioneering set of experiments performed by Lieber and co-workers a functionalised SFM tip, exposing a well-defined functional group at the tip surface, has been approached to a

surface holding a given unit. The measurements were done by recording force-distance curves while approaching the functionalised tip to the sample surface *via* a motion along the *Z*-axis (Fig. 5a). In this way the formation and rupture of a single supramolecular interaction was followed. This allowed the detection of the formation of H-bonds between COOH and COOH units, the presence of weaker interactions of van der Waals type between CH_3–CH_3 groups, and the existence of even weaker interactions between the dissimilar COOH and CH_3 moieties.[32] This kind of experiments can be done under vacuum, dry gas atmosphere or fluid. In this latter case, solvent effects normally play a key role in the interactions between the functional groups. For example, two COOH moieties exhibited long-range repulsions due to the presence of electrostatic interactions between the COO^- units in water, and short-range attractions caused by the formation of H-bonds in hexane.[33] By measuring the force-distance curves between identical units, including COOH, CH_3, OH, and NH_2, changing systematically the pH of the solution, a titration on the nanoscale was done. The determined pK_a was found to match the values obtained by conventional contact angle wetting studies of the same surfaces.[34]

More complex weak interactions, such as cation–ligand complexation between 18-crown-6 attached to the tip, and ammonium ions linked to the substrate surface were studied by CFM under ethanol. The specific complexation was suppressed by free potassium ion in the measurement solution, indicating a blocking effect based on the competitive

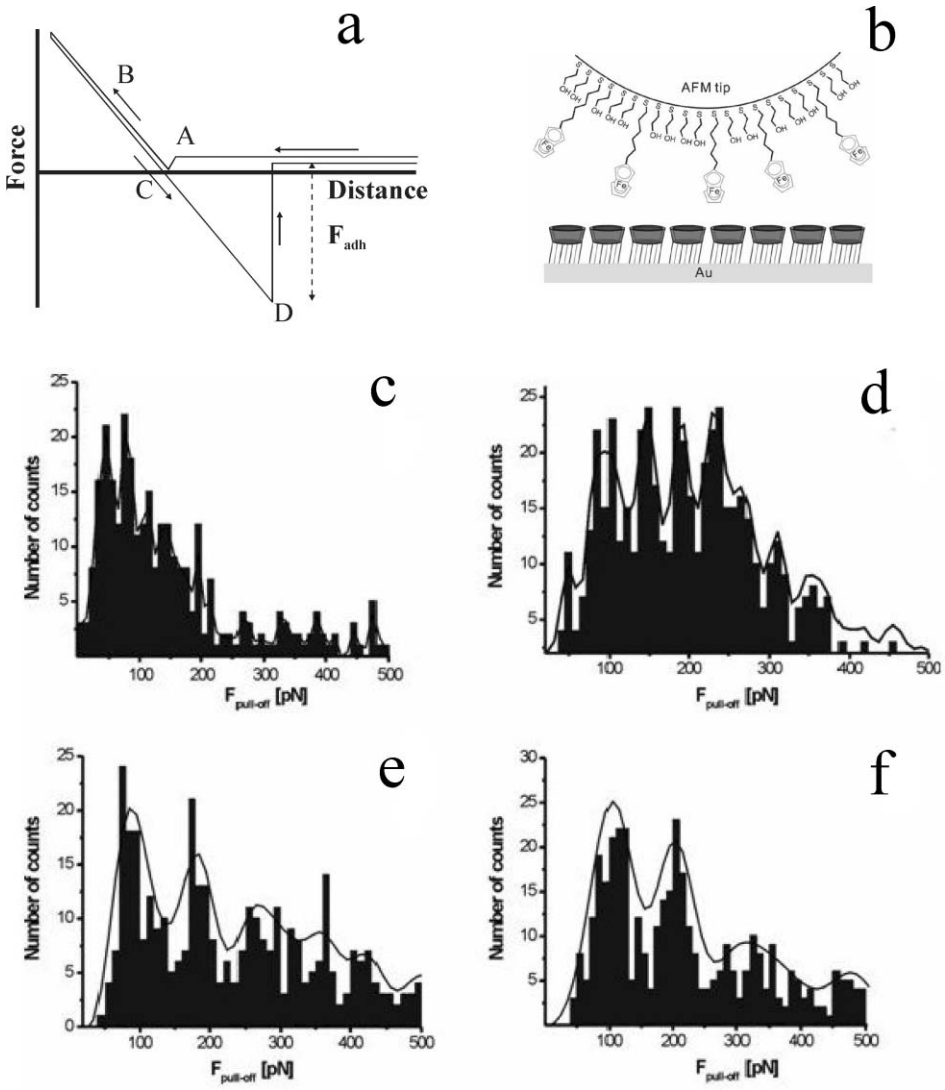

Fig. 5 (a) Force–distance curve collected by chemical force microscopy with the tip approaching the surface. At position A the tip is attracted to the surface. Decreasing the tip–sample distance, a repulsive regime (B,C) is reached. Pulling the tip away from the surface, a minimum (D) in the force–distance curve occurs characterised by a maximisation of the tip–surface adhesion due to capillary forces. Continuing the retraction, the tip breaks free from surface attraction. The tip, coated with a Au layer, is derivatised with alkanethiols bearing given functional groups in the ω-position, such as hydroxyl terminated alkanethiols and ferrocene functionalized alkanethiols. The sample surface is coated with a self-assembled monolayer exposing a different functionality, *i.e.* β-cyclodextrin heptathioether self-assembled on Au. (c–f) Histograms for the interactions of such a coated sample surface with a tip coated with 1% of (c) anilyl-, (d) toluidyl-, (e) *tert*-butylphenyl-, and (f) adamantylthiols (bin size 8 pN). The solid lines represent the FFT-smoothed histograms.[36] Reproduced with the permission of the American Chemical Society.

complexation of the 8-crown-6 moiety between the free ion and the ammonium bound to the substrate. The single complexation force of 18-crown-6 with ammonium was determined to be 60 pN.[35]

The strength of a charge-transfer complex, was determined by investigating with CFM under $CHCl_3$ the association between an electron donor and an acceptor, *i.e.* *N*,*N*,*N*′,*N*′-tetramethylphenylenediamine (TMPD) and 7,7,8,8-tetracyanoquinodimethane (TCNQ), respectively. The rupture of the individual bond occurred at a loading force of (70 ± 15) pN.[37]

A much stronger charge-transfer complex was found between a tip modified with a trinitrofluorenone derivative and a surface exposing a 9-anthracenemethanol derivative. While the strength of single bonds amounted to (6.6 ± 3.5) nN in dodecane, it decreased down to (1.7 ± 0.5)nN under 1-methylnaphthalene which acted as inhibiting aromatic solvent.[38] This result is most surprising since such weak interactions turned out to be stronger than a covalent bond, like that between sulfur and gold, which was found to be (1.4 ± 0.3) nN.[39]

Host–guest interactions constitute one of the hallmarks of supramolecular chemistry. The rupture forces of individual β-cyclodextrin (β-CD)-ferrocene host–guest complexes in an aqueous medium have been studied by immobilizing a thiol-derivatized ferrocene-guest on the SFM tip and a heptasulfide β-CD on the flat solid substrate (Fig. 5b). The effects of the alkyl spacer length of the ferrocene adsorbates, the relative concentration of ferrocene in the mixed monolayer on the SFM tip, and the unloading rate on the observed molecular unbinding events were investigated. Depending on the concentration of ferrocene moieties on the SFM tip, multiple or predominantly single pull-off events were observed. A statistical analysis showed that the observed rupture forces are integer multiples of one fundamental force quantum of (55 ± 10) pN, which was ascribed to the rupture of a single host–guest complex.[40] Following this preliminary work, the rupture forces of many other individual host–guest complexes based on β-CD heptathioether complexed with anilyl, toluidyl, *tert*-butylphenyl, and adamantylthiols were studied by single molecule force spectroscopy. The histograms of the pull-off forces showed several maxima at equidistant forces, with force quanta characteristic for each guest of (39 ± 15), (45 ± 15), (89 ± 15), and (102 ± 15) pN, respectively (Fig. 5 d–f). This force quantum was found to be independent of the number of interacting host–guest pairs, independent of the spacer length, and independent of the unloading rate, indicating that the host–guest complex rupture forces were probed under conditions of thermodynamic equilibrium. Noteworthy, the force values followed the same trend as the free binding energy ΔG° measured for model guest compounds in solution or on β-CD monolayers, as determined by microcalorimetry and surface plasmon resonance measurements, respectively.[36]

The strength of metallo-supramolecular bonds can also be studied with single rupture measurements, in this case carried out by single molecules force spectroscopy. The bond formed between two 2,2′:6″,2′ terpyridine complexed with ruthenium(II) complex had a strength of 95 pN, having therefore a magnitude similar to the well-known biotin–streptavidin pair.[41]

The attempt to correlate CFM measurements with the topographical SFM imaging, obtained using the same derivatised tip, provided successful results on nanopatterned surfaces,[34] although it revealed a fast degradation of the tip, due to the presence of frictional forces between tip and surface during raster scanning. In parallel to these experimental efforts, theoretical modelling has been performed in order to describe CFM results, as recently reviewed in.[42]

Besides the notable importance of monitoring reactions and exploring the strength of non-covalent interactions under thermodynamic equilibrium conditions on the nanoscale, therefore allowing to determine the free binding energy of an individual weak interaction, one might foresee the use of these approaches to explore cooperative hierarchical interactions as a path to tailor new complex materials with pre-programmed properties, like the mechanical ones. In particular, it will be most intriguing to combine this approach with external stimuli, *e.g.* light excitation, to unravel complex interactions and related phenomena occurring in nature.

Nanopatterning and nanomanipulation

Controlling the fabrication of objects on a scale spanning from 1 to 100 nm is a great challenge since it opens a wide range of applications spanning from catalysis, to nanoelectronics to biomedicine. Soon after the invention of SPMs[2] and the observation of their ability to modify surfaces, the field of scanning probe based lithography took off. Several approaches based on SPM manipulations had been then introduced.[43] Besides the careful reposition of atoms or molecules one by one under UHV environments, nanostructures where developed using the SPM tip to scrape or oxidize the surfaces with a nanoscale precision. Nevertheless these latter are limited by the choice of materials that can be manipulated, *i.e.* metals or semiconductors, and by the multi-step procedure that needs to be employed.

A novel route to template the growth of multilayers starting from chemisorbed self-assembled monolayers was introduced by Sagiv and co-workers at the end of the 90's. The conductive tip of a SFM was employed to locally oxidize vinyl groups, exposed on the surface of a self-assembled monolayer of 18-nonadecenyltrichlorosilane (NTS) chemisorbed on a silicon wafer. This was accomplished by applying a bias voltage of 8–9 V (tip negative) using different conductive SFM probes. The oxidation of the hydrophobic vinyl NTS end-groups led to hydrophilic carboxylic acid units, NTS_{Ox}, which were then used as the ground floor for the chemisorption of n-octadecyltrichlorosilane (OTS). In this way, only in the oxidized areas a second self-assembled layer was grown on the top of the first monolayer. The same SFM was then used to collect topographical and friction images which confirmed the pre-programmed patterning. This approach made it possible to draw lines and islands of OTS with a 10 nm resolution (Fig. 6A).[45]

Exploiting an electrochemical approach the same authors were able to accomplish an *in situ* chemical fabrication of spatially defined metal structures on organic monolayer

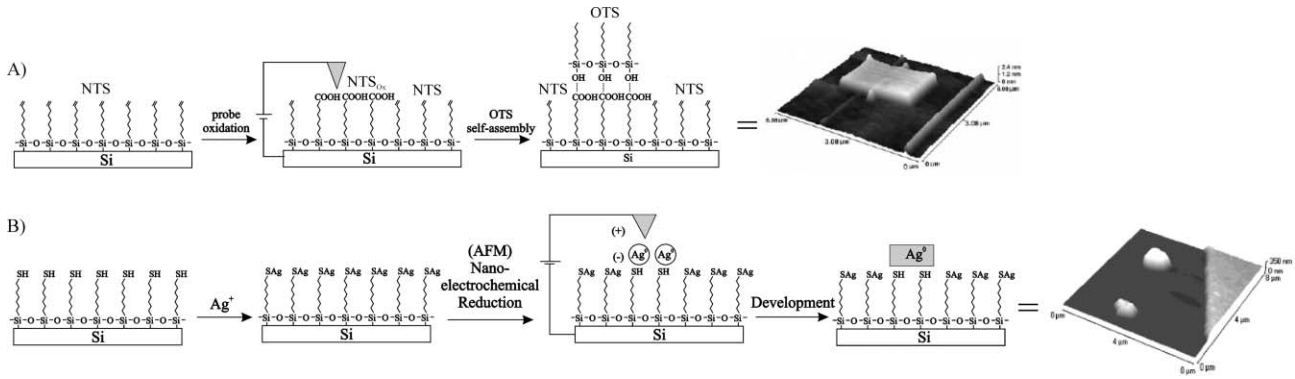

Fig. 6 Nanopatterning methodologies developed by Sagiv. (A) The vinyl units exposed on a monolayer of 18-nonadecenyltrichlorosilane (NTS) self-assembled on a Si wafer have been locally oxidized to carboxylic units (NTS_{Ox}). These latter have been used to template the subsequent self-assembly of a different chlorosilane, namely octadecyltrichlorosilane (OTS). The SFM shows the island of OTS on the flat NTS monolayer. (B) The SH moieties exposed on a thiol-top-functionalized silane monolayer (TFSM) self-assembled on a Si wafer have been transformed into SAg terminal units. The nanoelectrochemical reduction lead to Ag^0 atoms on the top of the SAM that can then be developed to obtain self-assembled silver islands selectively grown at tip-defined sites, as depicted in the SFM image.[44,45] Adapted with the permission of Wiley-VCH.

templates, such as a self-assembled monolayer, exposing some metallic silver nanodots, supported on a silicon wafer. Starting from a thiol top-functionalized silane monolayer (TFSM) with Ag^+ ions chemisorbed on its outer surface (Ag^+–TFSM), metallic silver nanoparticles were generated at selected surface sites by either wet chemical or tip-induced electrochemical reduction of the surface-bound metal ions (Fig. 6B).[44]

Following the same strategy of Fig. 6A, the second layer could expose a vinyl moiety ready to be either oxidized to a carboxylic acid or transformed into a thiol through the photo-induced radical addition of H_2S to the terminal ethylenic double bond. The reduction of the fraction of disulfide groups produced in the process with BH_3·THF followed. In this way different paths were pursued, which lead to the growth of a third layer made of either semiconducting (CdS) (Fig. 7A) or metallic (Ag or Au) (Fig. 7A,B) nanostructures, or chemisorbed alkylsilanes.[46] The transformation of the vinyl unit at the second floor into an amino group was obtained by photoreacting them with formamide and further reduction with BH_3·THF leading to the NH_2 function. This latter can guide the self-assembly of colloidal gold particles (Fig. 7C). This novel approach offers promising performance in terms of the precision, reproducibility, and structural robustness needed for the development of a reliable bottom-up nanofabrication methodology.[47]

In a different set of experiments, a SFM operating in contact mode has been used by Biscarini and co-authors to direct a mechanical perturbation on a layer of supramolecular engineered molecules, such as benzylic-amide-based rotaxanes. The localised effect at the contact area of the tip (Fig. 8) induces a local collective reorganisation of the material into spatially correlated nanodots. This phenomenon, which is due to the interconversion of rotaxanes in the solid state and to the formation and ripening of crystalline nuclei, takes place during the raster scanning of the SFM tip along a line with a load force just greater than a 2 nN threshold.[48] Although these

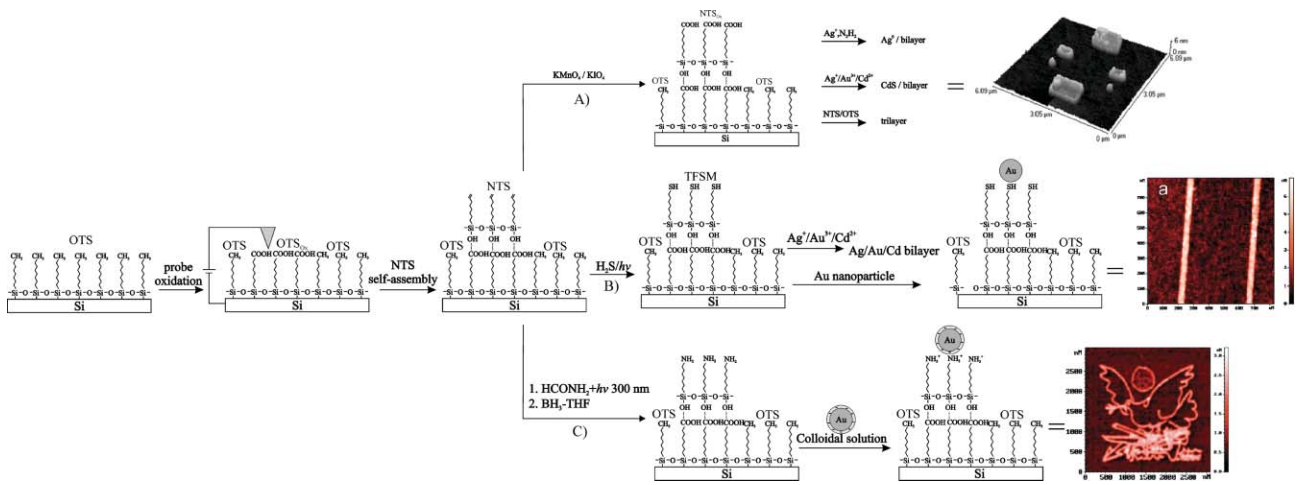

Fig. 7 (A) The methyl groups exposed on a monolayer of OTS self-assembled on a Si wafer have been locally oxidized to carboxylic units (OTS_{Ox}). These sites have templated the subsequent self-assembly of NTS, which expose a vinyl unit. The vinyl group was then (a) oxidized to a carboxylic function, (b) converted into a thiol unit or (c) transformed into an amino moiety. All three can be used as templates to grow metallic or semiconductor nanostructures.[46,47] Adapted with the permission of the American Chemical Society and Wiley-VCH.

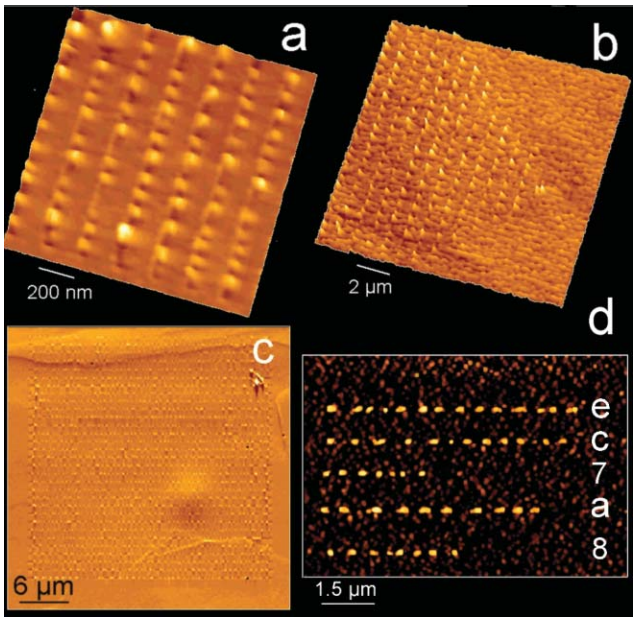

Fig. 8 (a) Array of points generated by scanning the SFM tip on a 5 nm-thick layer of benzylic-amide-based rotaxanes supported on HOPG. (b) For a given thickness (here 20 nm), the number of points is proportional to the scan length. The number of points can be estimated with a 2% accuracy. The film thickness governs the characteristic dimension of the points. Increasing the film thickness from 3 to 35 nm, the inter-point distance increases from 100 to 500 nm, the point full-width-at-half-maximum from 40 to 250 nm, and the point height from 1 to 20 nm, with a dispersion of 10 to 20%. (c) Pattern produced with 31 lines with 45 points each on a 30 × 30 μm^2 region on a thicker film. (d) Proof of concept for data storage: The sequence "e c 7 a 8" in the hexadecimal base corresponds to the number 968616.[48] Copyright 2003 AAAS (courtesy of Drs M. Cavallini and F. Biscarini).

manipulations were carried out on the (sub)micrometre scale, hence there was no exact control of conformational transitions at the single molecule level, these approaches might be extended to other species and on smaller length scales, using sharper tips and more space dependent manipulating conditions.

In the frame of nanopatterning and nanoconstruction at surfaces the invention of dip-pen nanolithography (DPN) by Mirkin and co-workers has been very valuable. DPN is a pretty simple and viable scanning-probe based direct-write tool for generating arbitrarily controlled surface pattern and chemical functionality with a resolution on the sub-hundred nanometre scale length. In this technique the SFM tip is used to deliver chemical species directly to nanoscopic regions of a given surface, *via* a solvent meniscus, which naturally forms in the ambient atmosphere (Fig. 9a). Similarly to a quill pen, the SFM tip is simply wet with a molecular 'ink' and then brought into contact with the surface to be patterned. Water condensing from the environment generates a capillary between the SFM tip and the surface, which in some cases assists the transfer of the ink onto the surface. In other cases, a physical or a chemical driving force, such as electrostatic interaction or chemisorption, aids the delivery of the ink from the tip to the substrate. In this way different nanostructures can be designed at surfaces, including spots, lines and curves.

DPN permitted to fabricate crystalline architectures of chemisorbed monolayers of 1-octadecanethiol and 16-mercaptohexadecanoic acid,[43] as well as to transfer to silicon oxide or modified silicon substrates, different dyes, including rhodamine 6G (R6G) (Fig. 9b),[50] coumarin 6 (C6), acid red 8 (AR8) and fluorescin (FITC). Fluorescence emission proved that the dye nanopatterns are optically active and the molecules are uniformly distributed within the pattern, opening perspectives for the use of this coloured ink DPN approach in high-density optical information storage, miniaturized optical devices and biological staining.[52]

Also polydisperse systems, *i.e.* poly[2-methoxy-5-2′-ethylhexyl)oxy-1,4-phenylenevinylene][50] and polythiophene[53] have been nanopatterned at surfaces making use of DPN. Due to the luminescence properties of such macromolecules, this result might be of interest for the future fabrication of a nanoscale light emitting diode (LED).

Different generations of starburst polyamidoamine dendrimers (PAMAM) and polypropylene imine dendrimers (DAB) have been delivered to the Si/SiO_x substrate by DPN. Features with a 100 nm size, consisting of approximately 20 DAB dendrimers, have been fabricated on the solid surface.[54]

A great advantage of DPN is the site-specific patterning of multiple inks at same location with high registry.

DPN has been also used to write patterns, using host–guest recognition, on molecular printboards. These latter are self-assembled monolayers of molecules that possess specific recognition sites, as molecular cavities, to which molecules

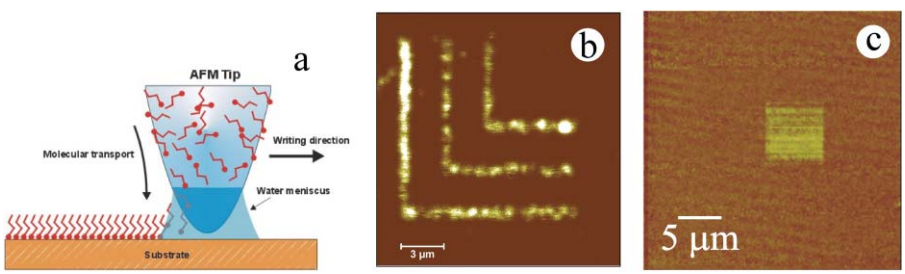

Fig. 9 Schematic representation of dip-pen nanolithography (DPN). (b) Scanning confocal microscopy image of Rhodamine 6G patterned by DPN in an array of lines on a glass surface. (c) SFM friction image of a pattern of bis(adamantly)-functionalized calixarene on a β-CD terminated SAM. Reprinted with permissions: (a) ref. 49 (Copyright 1999 AAAS), (b) ref. 50 from the American Chemical Society, (c) ref. 51 from Wiley-VCH.

can be anchored *via* specific and directional supramolecular interactions. On a print board consisting of β-CD derivatives, molecular patterns of calixarenes (Fig. 9c), dendritic wedges labelled with fluorescent dyes and dendrimers have been attached by DPN with a resolution below 100 nm. The advantage of this methodology lies in the tunability of the type and number of host–guest motifs and the possibility to erase patterns.[51]

This direct-write technique has been successfully employed to a number of molecular and biomolecular 'inks' on a variety of substrate types such as metals, semiconductors, and monolayer functionalised surfaces, thereby tailoring nanostructures composed of biological, organic, semiconducting, or metallic materials with controlled and well-defined nanometer shape and size, as very recently reviewed by Mirkin and coworkers.[55] This powerful approach seems to be ideal to nanoconstruct multicomponents 3D architectures with a controlled geometry.

Future perspectives

The use of SFM to study the supramolecular world is still in its infancy, thus there are plenty of unsolved issues to be tackled. The generation of more and more complex supramolecular architectures in the years to come will require more and more sophisticated set-ups and measurements to disentangle complex structures and behaviours. From the technological view point far more needs to be done to implement SFM instrumentation and modes that allow to achieve more precise quantitative determination of physico-chemical properties, including force interactions, electrical properties, *etc*.

The SFM visualization in real-time can be used to unravel supramolecular reactions and phenomena at solid–liquid interfaces. This might include the formation of supramolecular networks, casting light onto the kinetics and thermodynamics governing the process, the switching between different self-assembled motifs controlled by external stimuli, and the self-repair or self-healing of supramolecular arrangements.

The combination of SFM with a set-up offering optical characterization allowed to correlate structural and optical properties of supramolecular nanostructures. This was already done making use of scanning near field optical microscopy (SNOM) which combines both the possibilities of SFM and optical microscopy. The fluorescence of organic architectures, *i.e.* porphyrin rings with diameters spanning from 100 nm to 10 μm, was studied at the sub-micrometre scale and the probe of the SNOM was used to photo-induce a local modification on the ring.[56] Very recently, a combined force and optical microscope has made it possible to study at the single molecule level the properties of a new class of rigid multichromophoric polymers, *viz.* perylene polyisocyanides, which are expected to act as synthetic antennas. Two different structures have been found at surfaces: short non-helical perylene oligomers displaying monomer-like fluorescence properties, and a long helical perylene polymer exhibiting an emission which arises from multiple and independent excimer-like sites.[57] These studies paved the way towards the simultaneous exploration of the optical and structural properties of more and more complex supramolecular architectures. Moreover these set-ups might allow a variety of phenomena triggered by light to be followed.

Nanopatterning with SFM based approaches, as the local oxidation of Si surfaces, permits the fabrication of nanostructured surfaces which can be the playground for templating the self-assembly of supramolecular architectures. The possibility of using this nanopatterned surface to direct the growth of 2D architectures, *i.e.* a monolayer of sexithiophenes, opens perspectives to employ surface recognition to implant host molecules arbitrarily on the oxidized part,[58] thus to promote the formation of complex 3D supramolecular architectures at preset positions.

Nanomanipulation experiments, similar to those performed on single polymeric chains,[59] may allow to probe the mechanical properties of supramolecular architectures and to construct more and more complex species *via* reactions at surfaces, which could combine formation of covalent and non-covalent bonds in a hierarchical fashion. The use of SFM combined with external stimuli (light, pH, applied voltage) makes it possible to explore as many physico-chemical phenomena in both artificial and natural systems and permit the nanopatterning and nanomanipulation of surfaces.

Conclusions

The supramolecular approach, which is based on controlling the self-assembly of one or more components into highly ordered and complex supramolecular architectures, is essential to the improvement of nanotechnology. Scanning force microscopy-based methodologies are ultimate tools for the optimization of the bottom-up fabrication of multifaceted structures due to their applicability across a wide range of length scales, making it possible to cast light onto the hierarchy of interactions. Moreover they allow not only the visualization of surfaces, but also the study of numerous physico-chemical properties of tailor-made architectures. They have indisputably widened the scope of microscopy to address and tune the properties of single molecules and their controlled hierarchical self-assembly into complex functional 3D architectures. In the future, SFM will surely provide fundamental help to control the ever increasing complexity in self-assembled structures, thus paving the way for the fabrication of new supramolecular materials and devices with unpredictable properties and unexpectedly high performance.

Acknowledgements

Financial support from ESF-SONS-BIONICS, the EU through the Marie Curie EST project SUPER and the Force Tool project (NMP4-CT-2004-013684) is gratefully acknowledged. I wish to thank Dr Fabio Biscarini (Bologna) for introducing me to the fascinating world of scanning force microscopies. I owe much to Prof. Jürgen P. Rabe (Berlin) for his outstanding scientific guidance during the years I have spent in his group as well as for allowing me to deepen my knowledge of scanning probe microscopies and to their use to provide insight into physico-chemical properties of nanofunctional materials. I also would like to express my gratitude to long-term collaborators: Professors Klaus Müllen (Mainz),

Roeland J. M. Nolte and Alan E. Rowan (Nijmegen), Franco Cacialli (London), Giovanni Marletta (Catania). Moreover I thank my co-workers Drs Vincenzo Palermo, Pieter de Witte, Laura Sardone and Matteo Palma for enlightening discussions and comments on the manuscript.

Paolo Samorì†[ab]
[a]*Istituto per la Sintesi Organica e la Fotoreattività- Consiglio Nazionale delle Ricerche, via Gobetti 101, I-40129 Bologna, Italy. E-mail: samori@isof.cnr.it; Fax: +39 051 6399844*
[b]*Nanochemistry Laboratory – Institut de Science et d'Ingénierie Supramoléculaires (I.S.I.S.) -Université Louis Pasteur, 8, allée Gaspard Monge, F-67083 Strasbourg Cedex, France*

References

1 *Science*, 2002, vol. **295**, p. 2396, special issue on "Supramolecular Chemistry and Self-Assembly".
2 G. Binnig, H. Rohrer, C. Gerber and E. Weibel, *Helv. Phys. Acta*, 1982, **55**, 726.
3 G. Binnig, C. F. Quate and C. Gerber, *Phys. Rev. Lett.*, 1986, **56**, 930.
4 P. Samorì, V. Francke, K. Müllen and J. P. Rabe, *Chem. – Eur. J.*, 1999, **5**, 2312.
5 P. Leclère, A. Calderone, D. Marsitzky, V. Francke, Y. Geerts, K. Müllen, J. L. Brédas and R. Lazzaroni, *Adv. Mater.*, 2000, **12**, 1042.
6 C. Bustamante and D. Keller, *Phys. Today*, 1995, **48**, 32.
7 P. Leclère, E. Hennebicq, A. Calderone, P. Brocorens, A. C. Grimsdale, K. Müllen, J. L. Brédas and R. Lazzaroni, *Prog. Polym. Sci.*, 2003, **28**, 55.
8 J. M. Xu, C. Z. Zhou, L. H. Yang, N. T. S. Chung and Z. K. Chen, *Langmuir*, 2004, **20**, 950.
9 A. Schenning, A. F. M. Kilbinger, F. Biscarini, M. Cavallini, H. J. Cooper, P. J. Derrick, W. J. Feast, R. Lazzaroni, P. Leclère, L. A. McDonell, E. W. Meijer and S. C. J. Meskers, *J. Am. Chem. Soc.*, 2002, **124**, 1269.
10 Y. H. Luo, H. W. Liu, F. Xi, L. Li, X. G. Jin, C. C. Han and C. M. Chan, *J. Am. Chem. Soc.*, 2003, **125**, 6447.
11 D. J. Liu, H. Zhang, P. C. M. Grim, S. De Feyter, U. M. Wiesler, A. J. Berresheim, K. Müllen and F. C. De Schryver, *Langmuir*, 2002, **18**, 2385.
12 A. S. Drager, R. A. P. Zangmeister, N. R. Armstrong and D. F. O'Brien, *J. Am. Chem. Soc.*, 2001, **123**, 3595.
13 G. Gottarelli, S. Masiero, E. Mezzina, S. Pieraccini, J. P. Rabe, P. Samorì and G. P. Spada, *Chem. – Eur. J.*, 2000, **6**, 3242.
14 W. S. Yang, X. D. Chai, L. F. Chi, X. D. Liu, Y. W. Cao, R. Lu, Y. S. Jiang, X. Y. Tang, H. Fuchs and T. J. Li, *Chem. – Eur. J.*, 1999, **5**, 1144.
15 H. J. van Manen, V. Paraschiv, J. J. Garcia-Lopez, H. Schönherr, S. Zapotoczny, G. J. Vancso, M. Crego-Calama and D. N. Reinhoudt, *Nano Lett.*, 2004, **4**, 441.
16 E. Menozzi, R. Pinalli, E. A. Speets, B. J. Ravoo, E. Dalcanale and D. N. Reinhoudt, *Chem. – Eur. J.*, 2004, **10**, 2199.
17 B. H. Huisman, H. Schönherr, W. T. S. Huck, A. Friggeri, H. J. van Manen, E. Menozzi, G. J. Vancso, F. C. J. M. van Veggel and D. N. Reinhoudt, *Angew. Chem., Int. Ed.*, 1999, **38**, 2248.
18 N. Severin, J. Barner, A. A. Kalachev and J. P. Rabe, *Nano Lett.*, 2004, **4**, 577.
19 G. Podoprygorina, J. Zhang, V. Brusko, M. Bolte, A. Janshoff and V. Böhmer, *Org. Lett.*, 2003, **5**, 5071.
20 D. G. Kurth, N. Severin and J. P. Rabe, *Angew. Chem., Int. Ed.*, 2002, **41**, 3681.
21 N. Severin, J. P. Rabe and D. G. Kurth, *J. Am. Chem. Soc.*, 2004, **126**, 3696.
22 F. Cacialli, J. S. Wilson, J. J. Michels, C. Daniel, C. Silva, R. H. Friend, N. Severin, P. Samorì, J. P. Rabe, M. J. O'Connell, P. N. Taylor and H. L. Anderson, *Nat. Mater.*, 2002, **1**, 160.
23 P. Lo Nostro, A. Santoni, M. Bonini and P. Baglioni, *Langmuir*, 2003, **19**, 2313.
24 S. S. Sheiko and M. Möller, *Chem. Rev.*, 2001, **101**, 4099.
25 A. D. Schlüter and J. P. Rabe, *Angew. Chem., Int. Ed.*, 2000, **39**, 864.
26 C. Rivetti, M. Guthold and C. Bustamante, *J. Mol. Biol.*, 1996, **264**, 919.
27 P. Samorì, C. Ecker, I. Gössl, P. A. J. de Witte, J. J. L. M. Cornelissen, G. A. Metselaar, M. B. J. Otten, A. E. Rowan, R. J. M. Nolte and J. P. Rabe, *Macromolecules*, 2002, **35**, 5290.
28 T. W. Kelley, E. L. Granstrom and C. D. Frisbie, *Adv. Mater.*, 1999, **11**, 261.
29 A. Salomon, D. Cahen, S. Lindsay, J. Tomfohr, V. B. Engelkes and C. D. Frisbie, *Adv. Mater.*, 2003, **15**, 1881.
30 X. D. Cui, A. Primak, X. Zarate, J. Tomfohr, O. F. Sankey, A. L. Moore, T. A. Moore, D. Gust, G. Harris and S. M. Lindsay, *Science*, 2001, **294**, 571.
31 M. Nonnenmacher, M. P. Oboyle and H. K. Wickramasinghe, *Appl. Phys. Lett.*, 1991, **58**, 2921.
32 C. D. Frisbie, L. F. Rozsnyai, A. Noy, M. S. Wrighton and C. M. Lieber, *Science*, 1994, **265**, 2071.
33 T. Han, J. M. Williams and T. P. Beebe, Jr., *Anal. Chim. Acta*, 1995, **307**, 365.
34 D. V. Vezenov, A. Noy, L. F. Rozsnyai and C. M. Lieber, *J. Am. Chem. Soc.*, 1997, **119**, 2006.
35 S. Kado and K. Kimura, *J. Am. Chem. Soc.*, 2003, **125**, 4560.
36 T. Auletta, M. R. de Jong, A. Mulder, F. C. J. M. van Veggel, J. Huskens, D. N. Reinhoudt, S. Zou, S. Zapotoczny, H. Schönherr, G. J. Vancso and L. Kuipers, *J. Am. Chem. Soc.*, 2004, **126**, 1577.
37 H. Skulason and C. D. Frisbie, *J. Am. Chem. Soc.*, 2002, **124**, 15125.
38 R. Gil, J. C. Fiaud, J. C. Poulin and E. Schulz, *Chem. Commun.*, 2003, 2234.
39 M. Grandbois, M. Beyer, M. Rief, H. Clausen-Schaumann and H. E. Gaub, *Science*, 1999, **283**, 1727.
40 S. Zapotoczny, T. Auletta, M. R. de Jong, H. Schönherr, J. Huskens, F. C. J. M. van Veggel, D. N. Reinhoudt and G. J. Vancso, *Langmuir*, 2002, **18**, 6988.
41 M. Kudera, C. Eschbaumer, H. E. Gaub and U. S. Schubert, *Adv. Funct. Mater.*, 2003, **13**, 615.
42 P. Samorì, *J. Mater. Chem.*, 2004, **14**, 1353.
43 D. Wouters and U. S. Schubert, *Angew. Chem., Int. Ed.*, 2004, **43**, 2480.
44 R. Maoz, E. Frydman, S. R. Cohen and J. Sagiv, *Adv. Mater.*, 2000, **12**, 424.
45 R. Maoz, S. R. Cohen and J. Sagiv, *Adv. Mater.*, 1999, **11**, 55.
46 R. Maoz, E. Frydman, S. R. Cohen and J. Sagiv, *Adv. Mater.*, 2000, **12**, 725.
47 S. T. Liu, R. Maoz and J. Sagiv, *Nano Lett.*, 2004, **4**, 845.
48 M. Cavallini, F. Biscarini, S. León, F. Zerbetto, G. Bottari and D. A. Leigh, *Science*, 2003, **299**, 531.
49 R. D. Piner, J. Zhu, F. Xu, S. H. Hong and C. A. Mirkin, *Science*, 1999, **283**, 661.
50 A. Noy, A. E. Miller, J. E. Klare, B. L. Weeks, B. W. Woods and J. J. DeYoreo, *Nano Lett.*, 2002, **2**, 109.
51 T. Auletta, B. Dordi, A. Mulder, A. Sartori, S. Onclin, C. M. Bruinink, M. Peter, C. A. Nijhuis, H. Beijleveld, H. Schönherr, G. J. Vancso, A. Casnati, R. Ungaro, B. J. Ravoo, J. Huskens and D. N. Reinhoudt, *Angew. Chem., Int. Ed.*, 2004, **43**, 369.
52 M. Su and V. P. Dravid, *Appl. Phys. Lett.*, 2002, **80**, 4434.
53 Y. Li, B. W. Maynor and J. Liu, *J. Am. Chem. Soc.*, 2001, **123**, 2105.
54 R. McKendry, W. T. S. Huck, B. Weeks, M. Florini, C. Abell and T. Rayment, *Nano Lett.*, 2002, **2**, 713.
55 D. S. Ginger, H. Zhang and C. A. Mirkin, *Angew. Chem., Int. Ed.*, 2004, **43**, 30.
56 S. De Feyter, J. Hofkens, M. Van der Auweraer, R. J. M. Nolte, K. Müllen and F. C. De Schryver, *Chem. Commun.*, 2001, 585.
57 J. Hernando, P. A. J. de Witte, E. M. H. P. van Dijk, J. Korterik, R. J. M. Nolte, A. E. Rowan, M. F. García-Parajó and N. F. van Hulst, *Angew. Chem., Int. Ed.*, 2004, **43**, 4045.
58 R. Garcia, M. Tello, J.-F. Moulin and F. Biscarini, *Nano Lett.*, 2004, **4**, 1115.
59 J. Barner, F. Mallwitz, L. J. Shu, A. D. Schlüter and J. P. Rabe, *Angew. Chem., Int. Ed.*, 2003, **42**, 1932.